International Journal of Numerical Methods for Heat & Fluid Flow

Heat and mass transfer characteristics of MHD three-dimensional flow over a stretching sheet filled with water-based alumina nanofluid

P. Sudarsan A. Reddy, A. Chamkha,

Received 17 February 2017
Revised 21 April 2017
12 May 2017
Accepted 13 May 2017

Heat and mass transfer characteristics of MHD three-dimensional flow over a stretching sheet filled with water-based alumina nanofluid

P. Sudarsan A. Reddy
Department of Mathematics, RGM Engineering College, Nandyal, A.P., India, and
A. Chamkha
Department of Mechanical Engineering, Prince Mohammad Bin Fahd University, Al-Khobar, Saudi Arabia

Abstract

Purpose – This paper aims to understand the influence of velocity slip, nanoparticle volume fraction, chemical reaction and non-linear thermal radiation on MHD three-dimensional heat and mass transfer boundary layer flow over a stretching sheet filled with water-based alumina nanofluid. To get more meaningful results, the authors have taken nonlinear thermal radiation in the heat transfer process.

Design/methodology/approach – Suitable similarity variables are introduced to convert governing partial differential equations into the set of ordinary differential equations, and are solved numerically using a versatile, extensively validated finite element method with Galerkin's weighted residual simulation. The velocity, temperature and concentration profiles of nanoparticles as well as skin friction coefficient, Nusselt number and Sherwood number for different non-dimensional parameters such as volume fraction, magnetic, radiation and velocity slip parameters as well as the Prandtl number are examined in detail, and are presented through plots and tables.

Findings – It is noticed that the rate of heat transfer enhances with higher values of nanoparticle volume fraction parameter. It is worth mentioning that the heat transfer rates improve as the values of increase. Increasing values of M, R, θ_w and β decelerates the thickness of the thermal boundary layer in the fluid regime. The heat transfer rates decelerate as the values of suction parameter increase.

Originality/value – The authors have written this paper based on the best of their knowledge on heat and mass transfer analysis of nanofluids. The information in this paper is new and not copied from any other sources.

Keywords MHD, Non-linear thermal radiation, Velocity slip, Al_2O_3-water nanofluid, Chemical reaction, Three-dimensional fluid

Paper type Research paper

Nomenclature

C_p = specific heat at constant pressure;
k_s = thermal conductivity of nanoparticle;
ϕ_w = uniform constant concentration;
ϕ_∞ = free stream concentration;
K = permeability parameter;
M = magnetic parameter;

International Journal of Numerical Methods for Heat & Fluid Flow
Vol. 28 No. 3, 2018
pp. 532-546

0961-5539
DOI 10.1108/HFF-02-2017-0061

Nu_x = Nusselt number;
Pr = Prandtl number;
Sc = Schmidt number;
Sh_x = Sherwood number;
q_r = radiative heat flux;
T = temperature of the fluid;
T_w = uniform constant temperature;
T_∞ = free stream temperature;
k_0 = rate of chemical reaction;
u = velocity in the *x*-direction;
v = velocity in the y-direction;
w = velocity in the *z*-direction;
C_{fx} = skin-friction coefficient in *x*-direction;
C_{fx} = skin-friction coefficient in y-direction;
K^* = mean absorption coefficient;
(x, y, *z*) = Cartesian coordinates;
R = radiation parameter;
θ_w = temperature parameter;
ϕ = nanoparticle volume fraction;
a = stretching rate(constant);
Re_x = local Reynolds number in x –direction;
Re_y = local Reynolds number in y-direction; and
U_0 = suction parameter.

Greek symbols

θ = non-dimensional temperature;
μ_f = dynamic viscosity of the base fluid;
$(\mu)_{nf}$ = dynamic viscosity of the nanofluid;
η = dimensionless similarity variable;
ν_f = kinematic viscosity of the base fluid;
ρ_f = density of the base fluid;
ρ_{nf} = density of the nanofluid;
κ_f = thermal conductivity of base fluid;
$(\rho c_p)_{nf}$ = heat capacitance of the nanofluid;
φ = non-dimensional concentration;
σ = electrical conductivity;
σ^* = Stephan–Boltzmann constant;
γ = tangential momentum coefficient; and
λ = molecular free path.

Subscript

f = base fluid; and
nf = nanofluid.

1. Introduction

Nanofluids are formed by dispersing small volumetric quantities of nanometer-sized particles (1-100 nm) called nanoparticles in conventional heat transfer base fluids like water, ethylene glycol, toluene and engine oil. The nanoparticles used in nanofluids are typically made of metals (Al, Cu), oxides (Al_2O_3, CuO, TiO_2 and SiO_2), carbides

(SiC), nitrides (AlN and SiN) or nonmetals (graphite and carbon nanotubes). In recent years, the concept of a nanofluid has been proposed as route for enhancing the performance of the heat transfer rates in liquids. The materials that are in nanometer size possess unique physical and chemical properties. Choi *et al.* (2009) have proved in their experimental investigation that the thermal conductivity of the base fluid is enhanced approximately twice by dispersing nanoparticles with volume fraction of nanoparticles less than 1 per cent. In his benchmark study, Buongiorno (2006) reported seven possible mechanisms associating nanofluid natural convection through moment of nanoparticles in the base fluid using scale analysis. These mechanisms are nanoparticle size, inertia, particle agglomeration, Magnus effect, volume fraction of the nanoparticle, Brownian motion, particle size, thermophoresis, etc. Several authors, (Kakac and Pramuanjaroenkij, 2009; Kleinstreuer and Feng, 2011; Ozerinc *et al.*, 2010; Sundar *et al.*, 2013) have presented numerical and experimental studies to understand the thermal conductivity enhancement of the nanofluids. Nield and Kuznetsov (2009) extended the Cheng–Minkowycz problem for natural convection boundary layer heat and mass transfer flow through porous media filled with nanofluid. Kuznetsov and Nield (2010reported that Brownian motion and thermophoresis are very important in the thermal conductivity enhancement of nanofluid. Chamkha and Abu–Nada (2012), Chamkha and EL–Kabeir (2013), Chamkha and Ismael (2013) and Chamkha *et al.* (2014, 2015) presented the heat and mass transfer characteristics of nanofluid under the different geometries like single and doubled-driven square cavities, porous cavity heated by triangular thick wall, wedge and vertical cone, respectively.

The flow, heat and mass transfer problems over a stretching sheet through a porous medium is one of the important research areas in recent years because it is an important type of flow that occurs in many engineering and industrial disciplines, such as polymer technology, melt-spinning, hot rolling, wire drawing, glass–fiber production, manufacture of plastic and rubber sheets, cooling of a large metallic plate in a bath and continuous casting. In addition, many engineering process such as solar power technology, fossil fuel combustion energy process, astrophysical flows and space vehicle reentry at high temperatures involve a flow due to stretching surface. It is a well-known fact that magnetic field has specific applications in polymer processing technology. The stretching of plastic sheets in polymer industry, the cooling of continuous strips or filaments in metallurgy by drawing through an electrically conducting fluid, is subjected to the characteristics of the magnetic field. Magnetic nanoparticles are particularly convenient in biomedicine, sink float separation, cancer therapy, etc. Specific biomedical applications involving nanofluids include hyperthermia, magnetic cell separation, drug delivery and contrast enhancement in magnetic resonance imaging. Thermal radiation plays a very significant role in surface heat transfer when convection heat transfer is very small, and it has specific applications in the design of various innovative energy conversion systems working at high temperatures. Chemical reactions can be codified as either heterogeneous or homogeneous processes. This depends on whether they occur at an interface or as a single-phase volume reaction. In well-mixed systems, the reaction is heterogeneous if it takes place at an interface, and homogeneous if it takes place in solution. In most cases of chemical reactions, the reaction rate depends on the concentration of the species itself. A reaction is said to be of first order if the rate of reaction is directly proportional to the concentration itself. In many chemical engineering processes, a chemical reaction between a foreign mass and the fluid does occur. However, the diffusion process,

combined with homogeneous and/or heterogeneous chemical reactions of a particle in a porous medium, is also important in chemical engineering processes. In view of the above applications, Chamkha (2003), Chamkha and Aly (2011), Chamkha and EL–Kabeir (2013) and Chamkha and Ismael (2013) presented magneto hydro dynamics (MHD) heat and mass transfer behavior of nanofluid over a stretching sheet under the influence of various parameters such as radiation, chemical reaction and Soret and Dufour effects. Pal and Mondal (2011a, 2011b) analyzed the MHD boundary layer flow and heat and mass transfer of a fluid over a stretching sheet. Rana and Bhargava (2012) reported the flow and heat and mass transfer of nanofluid over a stretching sheet. Cheng (2013) has presented double-diffusive natural convection heat and mass transfer of a porous media saturated nanofluid over a vertical cone. Behseresht *et al.* (2014) have discussed heat and mass transfer characteristics of a nanofluid over a vertical cone using the practical range of thermo–physical properties of nanofluids. Recently, Ghalambaz *et al.* (2015) analyzed the influence of nanoparticle diameter and concentration on natural convection heat and mass transfer of Al_2O_3 – water-based nanofluids over a vertical cone. Kuznetstov and Neild (2014) reported natural convective boundary layer flow of a nanofluid over a vertical plate under different boundary conditions. Rashidi *et al.* (2014) analyzed the free convection boundary layer flow of a nanofluid over a stretching sheet. Sudarsana Reddy *et al.* (2017) perceived the heat transfer analysis of Ag–water and Cu–water nanofluids over rotating disk. Sreedevi *et al.* (2017) presented the influence of radiation and chemical reaction on heat and mass transfer characteristics of nanofluid over linear and non-linear stretching sheet. Heat and mass transfer analysis of nanofluids over different cavities are presented by Bondareva *et al.* (2015) and Sheremet *et al.*, (2016a, 2016b). Noghrehabadi *et al.* (2012a, 2012b, 2013 and 2014) discussed the natural convection heat transfer enhancement of nanofluids over different geometries. Pop *et al.* (2016) deliberated on free convection in a square porous cavity filled with a nanofluid using thermal non equilibrium and Buongiorno models.

To the best of the authors' knowledge, no studies have been found in literature to analyze the impact of velocity slip and non-linear thermal radiation on natural convection MHD three-dimensional heat and mass transfer nanofluid boundary layer flow over a stretching sheet in the presence of chemical reaction, so this problem is addressed here. The transformed boundary layer equations that represent the flow, temperature and concentration are solved numerically using the finite element method.

2. Mathematical formulation

Consider the steady, three-dimensional, viscous incompressible, laminar, MHD boundary layer flow of a nanofluid past a stretching sheet through nanofluid-saturated porous medium filled with water-based alumina nanofluid situated at $z = 0$. The coordinate system is chosen such that (u, v and w) be the velocity components along (x, y and z) directions, respectively. We also consider a constant magnetic field of strength B_0 in the z-direction. The flow is caused by the stretching of the sheet that moves in its own plane with the surface velocity ax, where a (stretching rate) is a positive constant. The stretching surface is maintained at a uniform temperature and concentration T_w and ϕ_w, and these values are assumed to be greater than the ambient temperature and concentration T_∞ and ϕ_∞, respectively. Under the above assumptions, the governing equations describing the momentum, energy and concentration in the presence of thermal radiation, chemical reaction take the following form:

$$\frac{\partial u}{\partial x}+\frac{\partial v}{\partial y}+\frac{\partial w}{\partial z}=0 \tag{1}$$

$$u\frac{\partial u}{\partial x}+v\frac{\partial u}{\partial y}+w\frac{\partial u}{\partial z}=\frac{\mu_{nf}}{\rho_{nf}}\frac{\partial^2 u}{\partial z^2}-\frac{\mu_{nf}}{\rho_{nf}}\frac{1}{K}u-\frac{1}{\rho_{nf}}\sigma_{nf}{B_0}^2u \tag{2}$$

$$u\frac{\partial v}{\partial x}+v\frac{\partial v}{\partial y}+w\frac{\partial v}{\partial z}=\frac{\mu_{nf}}{\rho_{nf}}\frac{\partial^2 v}{\partial z^2}-\frac{\mu_{nf}}{\rho_{nf}}\frac{1}{K}v-\frac{1}{\rho_{nf}}\sigma{B_0}^2v \tag{3}$$

$$u\frac{\partial T}{\partial x}+v\frac{\partial T}{\partial y}+w\frac{\partial T}{\partial z}=\alpha_{nf}\frac{\partial^2 T}{\partial z^2}-\frac{1}{(\rho c_p)_{nf}}\frac{\partial q_r}{\partial z} \tag{4}$$

$$u\frac{\partial \phi}{\partial x}+v\frac{\partial \phi}{\partial y}+w\frac{\partial \phi}{\partial z}=D_m\frac{\partial^2 \phi}{\partial z^2}-k_0(\phi-\phi_\infty) \tag{5}$$

The associated boundary conditions are as follows:

$$\begin{aligned} &u=ax+\frac{2-\gamma}{\gamma}\lambda\frac{\partial u}{\partial z},\ v=bx+\frac{2-\gamma}{\gamma}\lambda\frac{\partial v}{\partial z},\ w=-U_0,\ T=T_w,\ \phi=\phi_w,\ \text{at}\, z=0\\ &u\to 0,\quad v\to 0\qquad T\to T_\infty,\qquad \phi\to\phi_\infty,\qquad as\, z\to\infty. \end{aligned} \tag{6}$$

The dynamic viscosity μ_{nf}, density ρ_{nf}, thermal diffusivity α_{nf}, thermal conductivity k_{nf} heat capacitance $(\rho c_p)_{nf}$, electric conductivity σ_{nf} of the nanofluid and kinematic viscosity ν_f of the base fluid are defined as follows:

$$\begin{aligned} &\alpha_{nf}=\frac{k_{nf}}{(\rho c_p)_{nf}},\quad \mu_{nf}=\frac{\mu_f}{(1-\varphi)^{2.5}},\ \nu_f=\frac{\mu_f}{\rho_f},\quad \rho_{nf}=(1-\varphi)\rho_f+\varphi\rho_s,\\ &(\rho c_p)_{nf}=(1-\varphi)(\rho c_p)_f+\varphi(\rho c_p)_s,\frac{\sigma_{nf}}{\sigma_f}=1+\frac{3\left(\frac{\sigma_s}{\sigma_f}-1\right)\phi}{\left(\frac{\sigma_s}{\sigma_f}+2\right)-\left(\frac{\sigma_s}{\sigma_f}-1\right)\phi}\\ &k_{nf}=k_f\left(\frac{k_s+2k_f-2\varphi(k_f-k_s)}{k_s+2k_f+2\varphi(k_f-k_s)}\right). \end{aligned} \tag{7}$$

The similarity transformations are introduced as follows:

$$\begin{aligned} &u=axf'(\eta),\quad v=ayg'(\eta),\quad w=-\sqrt{a\nu_f}(f+g),\\ &\eta=\sqrt{\frac{a}{\nu_f}}z,\qquad \theta(\eta)=\frac{T-T_\infty}{T_w-T_\infty},\qquad S(\eta)=\frac{\phi-\phi_\infty}{\phi_w-\phi_\infty} \end{aligned} \tag{8}$$

By using Rosseland approximation for radiation, the radiative heat flux q_r is defined as under:

$$q_r = -\frac{4\sigma^*}{3K^*}\frac{\partial T^4}{\partial z} = -\frac{16\sigma^* T^3}{3K^*}\frac{\partial T}{\partial z} \tag{9}$$

The non-dimensional temperature $\theta(\eta) = \frac{T-T_\infty}{T_w-T_\infty}$ can be simplified as

$$T = T_\infty(1 + (\theta_w - 1)\theta) \tag{10}$$

where $\theta_w = \frac{T_w}{T_\infty}$ is the temperature parameter.

Using equations (8), (9) and (10), the governing non-linear partial differential equations (1)-(5), together with the boundary conditions (6) take the form the following:

$$f''' + A_1\left[(f+g)f'' - (f')^2\right] - k1f' - \frac{A_1}{A_2}Mf' = 0 \tag{11}$$

$$g''' + A_1\left[(f+g)g'' - (g')^2\right] - k1g' - \frac{A_1}{A_2}Mg' = 0 \tag{12}$$

$$\left(1+\frac{R}{A_4}\right)\theta'' + \Pr\frac{A_3}{A_4}(f+g)\theta' + \frac{R}{A_4}(\theta_w-1)^3\left(3\theta^2\theta'^2 + \theta^3\theta''\right) + \frac{3R}{A_4}(\theta_w-1)^2\left(2\theta\theta'^2 + \theta^2\theta''\right) + \frac{3R}{A_4}(\theta_w-1)\left(\theta'^2 + \theta\theta'\right) = 0 \tag{13}$$

$$S'' + Sc(f+g)S' - Sc\,Cr\,S = 0 \tag{14}$$

The transformed boundary conditions are as follows:

$$\begin{aligned} &\eta = 0,\ f'(0) = 1 + \beta f''(0),\ g'(0) = \alpha + \beta g''(0),\ f(0) + g(0) = V_0,\ \theta = 1,\ S = 1 \\ &\eta \to \infty,\quad f' = 0,\quad g'(0) = 0,\quad \theta = 0,\quad S = 0. \end{aligned} \tag{15}$$

where:
prime indicates ordinary differentiation with respect to η. In usual notations:

$Pr = \frac{\nu_f}{\alpha_f}$ (Prandtl number),

$M = \frac{\sigma B_0^2}{\rho_f a}$ (magnetic parameter),

$k1 = \frac{\nu_f}{K a}$ (porous parameter),

$Sc = \frac{\nu_f}{D_m}$ (Schmidt number),

$R = \frac{4T_\infty{}^3\sigma^*}{3K^*k}$ (Radiation parameter),

$\alpha = \frac{b}{a}$ (stretching rates ratio) $\beta = \frac{2-\gamma}{\gamma}\sqrt{\frac{a}{\nu_f}}\lambda$ (velocity slip parameter),

$V_0 = \frac{U_0}{\sqrt{a\nu_f}}$ (suction velocity),

$Cr = \frac{k_0}{a}$ (chemical reaction parameter). $A_1 = (1-\varphi) + \varphi\left(\frac{\rho_s}{\rho_f}\right)(1-\varphi)^{2.5}$,

$A_2 = (1-\varphi) + \varphi\left(\frac{\rho_s}{\rho_f}\right), A_3 = (1-\varphi) + \varphi\left(\frac{(\rho C_p)_s}{(\rho C_p)_f}\right), A_4 = \frac{k_{nf}}{k_f}$.

Quantities of practical interest in this problem are the local skin-friction coefficient along x and y directions, local Nusselt number and local Sherwood number. These are defined, respectively, as follows:

$C_{fx} = \frac{f''(0)}{(1-\varphi)^{2.5}Re_x^{\frac{1}{2}}}$, $C_{fy} = \frac{g''(0)}{(1-\varphi)^{2.5}Re_y^{\frac{1}{2}}}$, $Nu_x = -\left(1+R\theta_w^3\right)\theta'(0)\,Re_x^{\frac{1}{2}}$, $Sh_x = -S'(0)\,Re_x^{\frac{1}{2}}$. As the highly non-linear nature of ordinary differential equations (11)-(14), together with boundary conditions (15), they cannot be solved analytically. So the finite-element method (Bhargava *et al.*, 2009; Sudarsana Reddy and Chamkha, 2016a, 2016b, 2016c) has been implemented. The computer program of the algorithm was executed in Mathematica 10.0 software.

3. Numerical method of solution

3.1 The finite-element method

The finite-element method (FEM) is a very powerful method for solving ordinary differential equations and partial differential equations. The basic idea of this method is to divide the whole domain into smaller elements of finite dimensions called finite elements. This method is a very good numerical method in modern engineering analysis, and it can be applied for solving integral equations including heat transfer, fluid mechanics, chemical processing, electrical systems and many other fields. The steps involved in the FEM are as follows.

3.1.1 Finite-element discretization. In the finite element discretization, the entire interval is divided into a finite number of subintervals and this subinterval is called an element. The set of all these elements is called the finite-element mesh.

3.1.2 Generation of the element equations.

- Variational formulation of the mathematical model over the typical element (an element from the mesh) is performed.
- An approximate solution of the variational problem is assumed, and the element equations are made by substituting this solution in the above system.
- Using interpolating polynomials, the stiffness matrix is constructed.

3.1.3 Assembly of element equations. By imposing inter element continuity conditions all the algebraic equations are assembled. This result in a large number of algebraic equations called global FEM and it represents the whole domain.

3.1.4 Imposition of boundary conditions. The boundary conditions that represent the flow model are imposed on the assembled equations.

3.1.5 Solution of assembled equations. The assembled equations so obtained can be solved by any of the numerical techniques, namely, the Gauss elimination method, LU decomposition method, etc. An important consideration is that of the shape functions used to approximate actual functions. The entire flow domain is divided into 10,000 quadratic elements of equal size and every element is three-noded, so the entire domain contains 20,001 nodes. We have to evaluate four functions f, h, θ and S at every node. We

obtained 80,004 non-linear equations after the assembly of element equations. After applying the given boundary conditions, the remaining system of non-linear equations are solved by using the Gauss elimination method, while maintaining an accuracy of 0.00001. Gaussian quadrature is implemented for solving the integrations. The computer program of the algorithm was executed in MATHEMATICA 10.0 running on a PC. To investigate the sensitivity of the solutions to mesh density, we have performed the grid invariance test for velocity, temperature and concentration distributions, as shown in Table I. It is observed from this table that in the same domain, the accuracy is not affected, and even the number of elements increased by decreasing the size of the elements.

4. Results and discussion

Comprehensive numerical computations are conducted for different values of the parameters that describe the flow characteristics and the results are illustrated graphically. A representative set of computational results are presented in Figures 1-4. The thermo–physical properties of water and nanoparticles are shown in Table II. The comparison of the present results with the results reported by Hayat *et al.* [2015] has been made and found in good agreement, which is shown in Table III.

Figures 1(a)-(d) depict the velocity profiles along x and y directions for different values of nanoparticle volume fraction (ϕ), magnetic parameter (M), velocity slip parameter (β) and suction parameter (V_0). It is perceived from Figure 1(a) that both velocity profiles f' and g' are enhanced in Al_2O_3–water-based nanofluid as the nanoparticle volume fraction (ϕ) increases. This is because of the fact that increasing the nanoparticle volume fraction enhances the momentum boundary layer thickness in the flow regime. It is noticed that the velocity profiles f' and g' both decrease as the values of M increases in the boundary layer regime. This is owing to the fact that the presence of magnetic field in the flow creates a force known as the Lorentz force. which acts as a retarding force as a result the momentum boundary layer thickness decelerates throughout the flow region [Figure 1(b)]. Both velocity profiles f' and g' are diminutions as the values of velocity slip parameter β increases in the boundary layer regime. as shown in Figure 1(c). It is observed from Figure 1(d) that as the values of suction parameter increases, both the velocity profiles f' and g' decelerate in the fluid region. This is because suction is taken away the warm fluid from the surface of the sheet, thereby decreasing the thickness of the velocity boundary layer.

	f'				Θ				S			
	Step size (h)											
η	0.04	0.02	0.01	0.005	0.04	0.02	0.01	0.0005	0.04	0.02	0.01	0.0005
0.0	1.0000	1.0000	1.0000	1.0000	1.0000	1.0000	1.0000	1.0000	1.0000	1.0000	1.0000	1.0000
1.0	0.2095	0.1847	0.1846	0.1845	0.1881	0.1662	0.1457	0.1456	0.3210	0.2642	0.2217	0.2216
2.0	0.0822	0.0621	0.0620	0.0620	0.0102	0.0092	0.0070	0.0070	0.1025	0.0824	0.0752	0.0751
3.0	0.0306	0.0214	0.0213	0.0212	0.0002	0.0003	0.0003	0.0003	0.0282	0.0193	0.0161	0.0128
4.0	0.0101	0.0091	0.0090	0.0090	0.0000	0.0000	0.0000	0.0000	0.0069	0.0054	0.0042	0.0041
5.0	0.0002	0.0001	0.0001	0.0001	–	–	–	–	0.0029	0.0018	0.0014	0.0013
6.0	0.0000	0.0000	0.0000	0.0000	–	–	–	–	0.0019	0.0011	0.0010	0.0009
7.0	–	–	–	–	–	–	–	–	0.0002	0.0002	0.0002	0.0002
8.0	–	–	–	–	–	–	–	–	0.0000	0.0000	0.0000	0.0000

Table I. Grid-invariance test for velocity distribution (f'), temperature distribution (θ) and concentration distribution (ϕ)

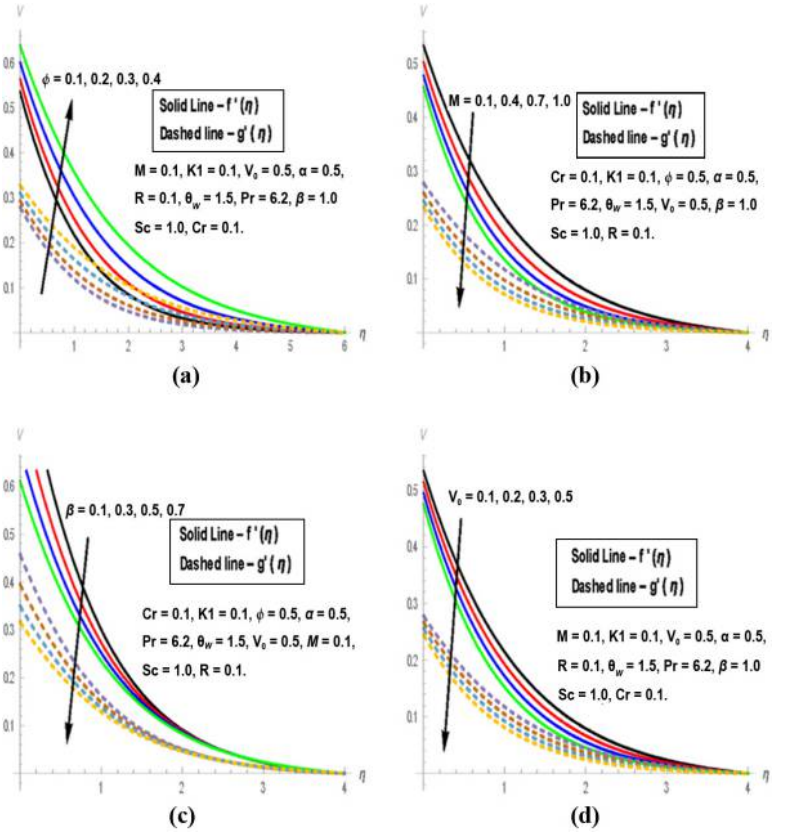

Figure 1.
Velocity profiles f' and g' for various values of (a) volume fraction parameter ϕ, (b) magnetic parameter M, (c) velocity slip parameter and (d) suction parameter

Figures 2(a)-(d) illustrates the influence of various parameters, nanoparticle volume fraction (ϕ), magnetic parameter (M), temperature parameter (θ_w) and radiation parameter (R) on temperature profiles. It is noticed from Figure 2(a) that the temperature profiles retards as the nanoparticle volume fraction increases. The temperature profiles elevate as the values of magnetic parameter increases [Figure 2(b)]. This is because the presence of magnetic field in an electrically conducting fluid produces a force called Lorentz force. To overcome the drag force imposed by the Lorentzian retardation, the fluid has to perform extra work; this supplementary work can be converted into thermal energy which increases the thickness of the thermal boundary layer. It is perceived from Figures 2(c) and (d) that as the values of temperature parameter and radiation parameter increases, the temperature profiles are also enhanced. This is because the mean absorption coefficient decreases with increasing values of radiation parameter; as a result the thermal boundary layer thickness of the fluid is rises.

The impact of suction parameter (V_0) and velocity slip parameter (β) on temperature profiles is plotted in Figures 3(a)-(b). It is seen from Figure 3(a) that the temperature profiles retards with higher values of (V_0). However, the thermal boundary layer thickness of the fluid is enhanced as the values of (β) increases.

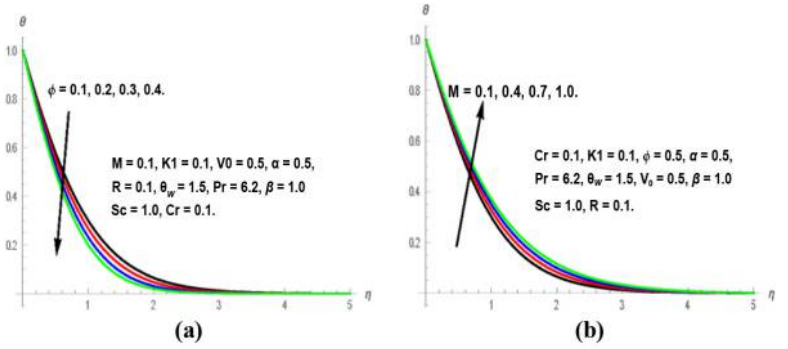

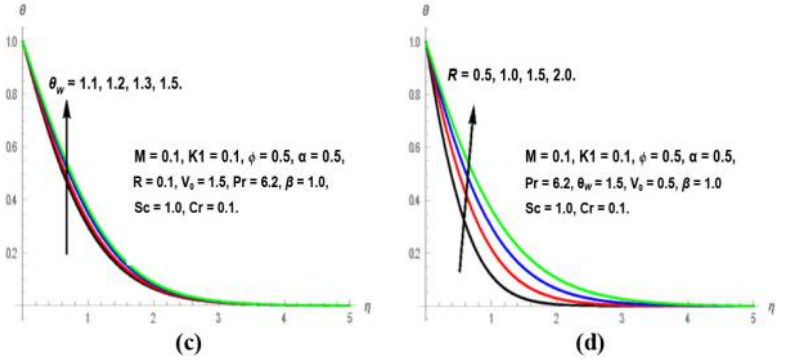

Figure 2.
Temperature profiles θ for various values of (a) volume fraction parameter ϕ, (b) magnetic parameter M, (c) temperature parameter and (d) radiation parameter

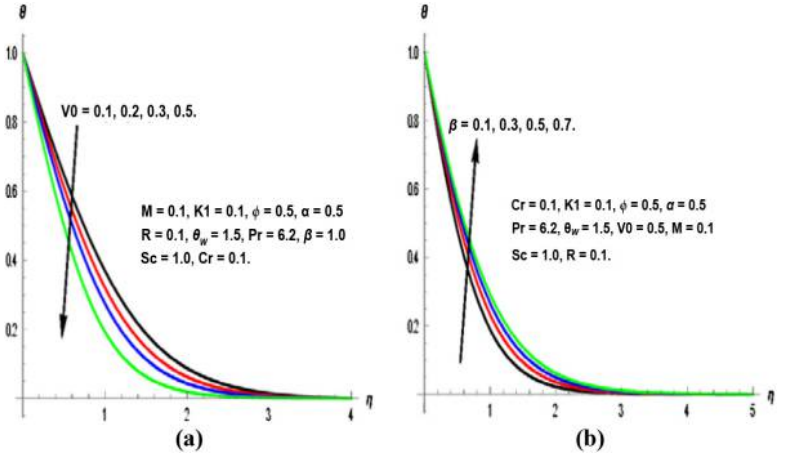

Figure 3.
Temperature profiles θ for various values of (a) suction parameter V_0 and (b) velocity slip parameter β

The concentration distributions for various values of nanoparticle volume fraction (ϕ), suction parameter (V_0), velocity slip parameter (β) and chemical reaction parameter (Cr) are depicted in Figures 4(a)-(d), respectively. It is noticed from Figures 4(a) and (b) that the concentration profiles decelerates with the increasing values of nanoparticle volume

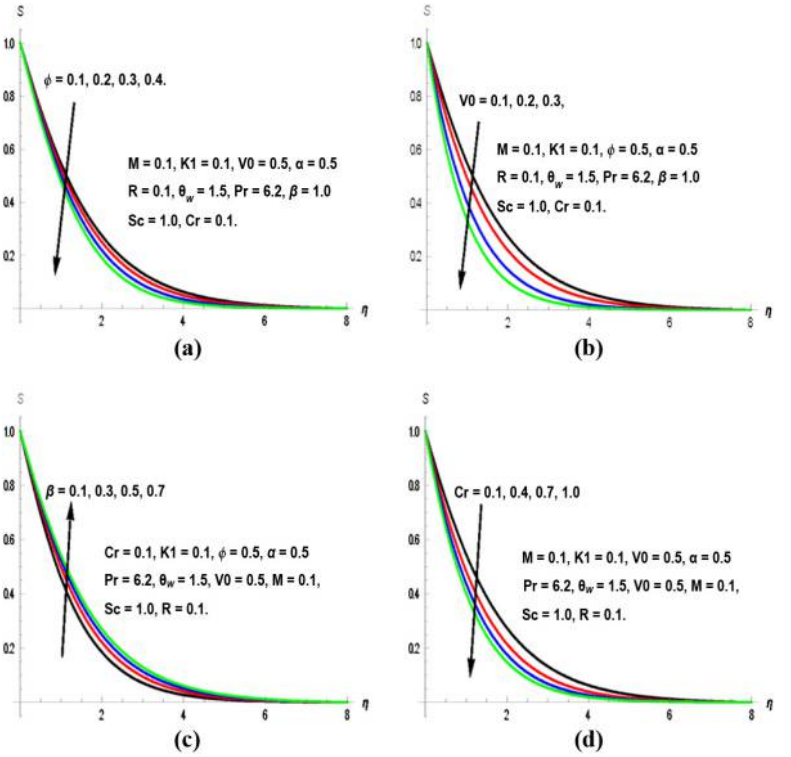

Figure 4.
Concentration profiles S for various values of (a) volume fraction parameter ϕ, (b) suction parameter V_0, (c) velocity slip parameter β and (d) chemical parameter cr

Fluid	$\rho\left(\frac{Kg}{m^3}\right)$	$C_p\left(\frac{J}{kgK}\right)$	$k\left(\frac{W}{mK}\right)$	$\beta \times 10^5 (K^{-1})$
Pure water	997.1	4,179	0.613	21
Copper (Cu)	8,933	385	401	1.67
Silver (Ag)	10,500	235	429	1.89
Alumina (Al_2O_3)	3,970	765	40	0.85
Titanium Oxide (TiO_2)	4,250	686.2	8.9538	0.9

Table II.
Thermo-physical properties of water and nanoparticles

fraction (ϕ) and suction parameter (V_0) in the Al_2O_3–water-based nanofluid. An increase in the values of velocity slip parameter (β) elevates the solutal boundary layer thickness in the boundary layer regime [Figure 4(c)]. We have seen from Figure 4(d) that the concentration profiles are highly influenced and impede with the chemical reaction parameter in the flow regime.

The values of skin-friction coefficient along x and y directions, Nusselt number and Sherwood number for the Al_2O_3–water based nanofluid are calculated and presented in Table IV. It is clear that the skin-friction coefficient along x and y direction has similar trend for different values of ϕ, β and V_0. The skin-friction coefficient along x and y direction are both enhanced with the increasing values of ϕ and β. However, they both

retards with higher values of suction parameter V_0. It is noticed that the rates of heat transfer are clearly enhanced with the higher values of ϕ. With the improving values of suction parameter V_0 amplify the heat transfer rates in the boundary layer regime. It is evident from Table IV that the rates of mass transfer are increased with increasing values of the both parameters ϕ and V_0, whereas s of Sherwood number with higher values of β.

5. Conclusion

In this article, we have studied natural convection boundary layer three-dimensional flow, heat and mass transfer of Al_2O_3–water-based nanofluid over a stretching sheet through porous medium by taking partial slip, suction, non-linear thermal radiation, magnetic field and chemical reaction into account. The momentum boundary layer thickness is elevated, whereas thermal boundary layer thickness decelerates with higher values of nanoparticle volume fraction parameter (ϕ). It is worth mention that the heat transfer rates improve as the values of ϕ increase. Increasing values of M, R, θ_w and β decelerates the thickness of the thermal boundary layer in the fluid regime. The heat transfer rates decelerate as the values of suction parameter increase.

Parameter			$-\theta'(0)$	
M	θ_w	R	Hayat *et al.* (2015)	Present study
0.1	1.1	0.1	0.74084	0.74081
0.3	1.1	0.1	0.70977	0.70975
0.5	1.1	0.1	0.68279	0.68281
0.1	1.2	0.1	0.74410	0.74413
0.1	1.3	0.1	0.74775	0.74776
0.1	1.4	0.1	0.75180	0.75182
0.1	1.1	0.05	0.73328	0.73329
0.1	1.1	0.15	0.74802	0.74801
0.1	1.1	0.2	0.75482	0.75483

Table III. Comparison of ($-\theta'$ (0)) with previously published data

φ	V_0	β	$f''(0)$	$g''(0)$	$-\theta'(0)$	$-S'(0)$
0.1	0.5	1.0	–0.465405	–0.221279	0.953875	0.538901
0.4	0.5	1.0	–0.437013	–0.207472	1.018023	0.562917
0.7	0.5	1.0	–0.399428	–0.189562	1.092812	0.594689
1.0	0.5	1.0	–0.361674	–0.172096	1.165039	0.625896
0.1	0.1	1.0	–0.465491	–0.221341	0.750102	0.543008
0.1	0.2	1.0	–0.485181	–0.232735	0.836987	0.615064
0.1	0.3	1.0	–0.504933	–0.244038	0.926619	0.692405
0.1	0.5	1.0	–0.543917	–0.265949	1.112660	0.861667
0.1	0.5	0.1	–0.949914	–0.429223	1.218382	0.665998
0.1	0.5	0.3	–0.763691	–0.351956	1.102273	0.608956
0.1	0.5	0.5	–0.642979	–0.300220	1.024832	0.571745
0.1	0.5	0.7	–0.557446	–0.262743	0.968601	0.545254

Table IV. The values of skin-friction coefficient ($f''(0)$) along x-direction, skin-friction coefficient ($g''(0)$) along y–direction, Nusselt number ($-\theta'(0)$) and Sherwood number ($-S'(0)$) for different values of ϕ, V_0 and β

References

Behseresht, A., Nogrehabadi, A. and Ghalambaz, M. (2014), "Natural-convection heat and mass transfer from a vertical cone in porous media filled with nanofluids using practical ranges of nanofluids thermo-physical properties", *Chemical Engineering Research and Design*, Vol. 92 No. 3, pp. 447-452.

Bhargava, R., Sharma, R. and Bég, O.A. (2009), "Oscillatory chemically-reacting MHD free convection heat and mass transfer in a porous medium with Soret and Dufour effects: finite element modeling", *International Journal of Applied Mathematics and Mechanics*, Vol. 5 No. 6, pp. 15-37.

Bondareva, N.S., Sheremet, M.A. and Pop, I. (2015), "Magnetic field effect on the unsteady natural convection in a right-angle trapezoidal cavity filled with a nanofluid: Buongiorno's mathematical model", *International Journal of Numerical Methods for Heat & Fluid Flow*, Vol. 25 No. 8, pp. 1924-1946.

Buongiorno, J. (2006), "Convective transport in nanofluids", *Journal of Heat Transfer*, Vol. 128 No. 3, pp. 240-250.

Chamkha, A.J. (2003), "MHD flow of a uniformly stretched vertical permeable surface in the presence of heat generation/absorption and a chemical reaction", *International Communications in Heat and Mass Transfer*, Vol. 30 No. 3, pp. 413-422.

Chamkha, A.J. and Abu-Nada, E. (2012), "Mixed convection flow in single- and double-lid driven square cavities filled with water-Al_2O_3 nanofluid: effect of viscosity models", *European Journal of Mechanics - B/Fluids*, Vol. 36, pp. 82-96.

Chamkha, A.J. and Aly, A.M. (2011), "Heat and mass transfer in stagnation-point flow of a polar fluid towards a stretching surface in porous media in the presence of Soret", *Dufour and Chemical Reaction Effects, Chemical Engineering Communications*, Vol. 198, pp. 214-234.

Chamkha, A.J. and EL-Kabeir, S.M. (2013), "Unsteady heat and mass transfer by MHD mixed convection flow over an impulsively stretched vertical surface with chemical reaction and soret and dufour effects", *Chemical Engineering Communications*, Vol. 200 No. 9, pp. 1220-1236.

Chamkha, A.J. and Ismael, M.A. (2013), "Conjugate heat transfer in a porous cavity filled with nanofluids and heated by triangular thick wall", *International Journal of Thermal Sciences*, Vol. 67, pp. 135-151.

Chamkha, A.J., Abbasbandy, S. and Rashad, A.M. (2015), "Non-darcy natural convection flow of non-newtonian nanofluid over a cone saturated in a porous medium with uniform heat and volume fraction fluxes", *International Journal of Numerical Methods for Heat & Fluid Flow*, Vol. 25 No. 2, pp. 422-437.

Chamkha, A.J., Rashad, A.M. and Gorla, R. (2014), "Non-similar solutions for mixed convection along a wedge embedded in a porous medium saturated by a non-newtonian nanofluid", *International Journal of Numerical Methods for Heat & Fluid Flow*, Vol. 24 No. 7, pp. 1471-1486.

Cheng, C.Y. (2013), "Double-diffusive natural convection from a vertical cone in a porous medium saturated with a nanofluid", *Journal of the Chinese Society of Mechanical Engineers*, Vol. 34, pp. 401-409.

Choi, S.U.S. and Eastman, J.A. (2009), "Enhancing thermal conductivities of fluids with nanoparticles", *Proceedings of the ASME International Mechanical Engineering Congress and Exposition*, Vol. 66, pp. 99-105.

Ghalambaz, M., Behseresht, A., Behseresht, J. and Chamkha, A.J. (2015), "Effect of nanoparticle diameter and concentration on natural convection in Al_2O_3 – water nanofluids considering variable thermal conductivity around a vertical cone in porous media", *Advanced Powder Technology*, Vol. 26 No. 1, pp. 224-235.

Hayat, T., Imtiaz, M., Alsaedi, A. and Kutbi, M.A. (2015), "MHD three-dimensional flow of nanofluid with velocity slip and nonlinear thermal radiation", *Journal of Magnetism and Magnetic Materials*, Vol. 396, pp. 31-37.

Kakac, S. and Pramuanjaroenkij, A. (2009), "Review of convective heat transfer enhancement with nanofluids", *International Journal of Heat and Mass Transfer*, Vol. 52 Nos 13/14, pp. 3187-3196.

Kleinstreuer, C. and Feng, Y. (2011), "Experimental and theoretical studies of nanofluid thermal conductivity enhancement: a review", *Nanoscale Research Letters*, Vol. 6, p. 229.

Kuznetsov, A.V. and Nield, D.A. (2010), "Natural convective boundary-layer flow of a nanofluid past a vertical plate", *International Journal of Thermal Sciences*, Vol. 49 No. 2, pp. 243-247.

Kuznetstov, A.V. and Neild, D.A. (2014), "Natural convective boundary-layer flow of a nanofluid past a vertical plate: a revised model", *International Journal of Thermal Sciences*, Vol. 77, pp. 126-129.

Nield, D.A. and Kuznetsov, A.V. (2009), "The cheng-minkowycz problem for natural convective boundary-layer flow in a porous medium saturated by a nanofluid", *International Journal of Heat and Mass Transfer*, Vol. 52 Nos 25/26, pp. 5792-5795.

Noghrehabadi, A., Ghalambaz, M. and Ghanbarzadeh, A. (2014), "Effects of variable viscosity and thermal conductivity on natural-convection of nanofluids past a vertical plate in porous media", *Journal of Mechanics*, Vol. 30 No. 3, pp. 265-275.

Noghrehabadi, A., Pourrajab, R. and Ghalambaz, M. (2012a), "Effect of partial slip boundary condition on the flow and heat transfer of nanofluids past stretching sheet prescribed constant wall temperature", *International Journal of Thermal Sciences*, Vol. 54, pp. 253-261.

Noghrehabadi, A., Ghalambaz, M., Ghalambaz, M. and Ghanbarzadeh, A. (2012b), "Comparing thermal enhancement of ag-water and SiO2-water nanofluids over an isothermal stretching sheet with suction or injection", *Journal of Computational & Applied Research in Mechanical Engineering*, Vol. 2, pp. 37-49.

Noghrehabadi, A., Saffarian, M.R., Pourrajab, R. and Ghalambaz, M. (2013), "Entropy analysis for nanofluid flow over a stretching sheet in the presence of heat generation/absorption and partial slip", *Journal of Mechanical Science and Technology*, Vol. 27 No. 3, pp. 927-937.

Ozerinc, S., Kakac, S. and Yazıcıoglu, A. (2010), "Enhanced thermal conductivity of nanofluids: a state-of-the-art review", *Microfluidics and Nanofluidics*, Vol. 8 No. 2, pp. 145-170.

Pal, D. and Mondal, H. (2011a), "Effects of soret, dufour, chemical reaction and thermal radiation on MHD non-darcy unsteady mixed convective heat and mass transfer over a stretching sheet", *Communications in Nonlinear Science and Numerical Simulation*, Vol. 16 No. 4, pp. 1942-1958.

Pal, D. and Mondal, H. (2011b), "MHD non-darcian mixed convection heat and mass transfer over a non-linear stretching sheet with soret and dufour effects and chemical reaction", *International Communications in Heat and Mass Transfer*, Vol. 38 No. 4, pp. 463-467.

Pop, I., Ghalambaz, M. and Sheremet, M. (2016), "Free convection in a square porous cavity filled with a nanofluid using thermal non equilibrium and buongiorno models", *International Journal of Numerical Methods for Heat & Fluid Flow*, Vol. 26, pp. 671-693.

Rana, P. and Bhargava, R. (2012), "Flow and heat transfer of a nano fluid over a nonlinearly stretching sheet: a numerical study", *Communications in Nonlinear Science and Numerical Simulation*, Vol. 17 No. 1, pp. 212-226.

Rashidi, M.M., Rostami, B., Freidoonimehr, N. and Abbasbandy, S. (2014), "Free convective heat and mass transfer for MHD fluid flow over a permeable vertical stretching sheet in the presence of the radiation and buoyancy effects", *Ain Shams Engineering Journal*, Vol. 5 No. 3, pp. 901-912.

Sheremet, M.A., Oztop, H.F. and Pop, I. (2016a), "MHD natural convection in an inclined wavy cavity with corner heater filled with a nanofluid", *The Journal of Magnetism and Magnetic Materials*, Vol. 416, pp. 37-47.

Sheremet, M.A., Pop, I. and Rosca, N.C. (2016b), "Magnetic field effect on the unsteady natural convection in a wavy-walled cavity filled with a nanofluid: Buongiorno's mathematical model", *Journal of the Taiwan Institute of Chemical Engineers*, Vol. 61, pp. 211-222.

Sreedevi, P., Sudarsana Reddy, P. and Chamkha, A.J. (2017), "Heat and mass transfer analysis of nanofluid over linear and non- linear stretching surface with thermal radiation and chemical reaction", *Powder Technology*, Vol. 315, pp. 194 -204.

Sudarsana Reddy, P. and Chamkha, A.J. (2016a), "Soret and dufour effects on MHD heat and mass transfer flow of a micropolar fluid with thermophoresis particle deposition", *Journal of Naval Architechure and Marine Engineering*, Vol. 13 pp. 39-50.

Sudarsana Reddy, P. and Chamkha, A.J. (2016b), "Soret and dufour effects on unsteady MHD heat and mass transfer over a stretching sheet with thermophoresis and non-uniform heat generation/absorption", *Journal of Applied Fluid Mechanics*, Vol. 9 No. 7, pp. 2443-2455.

Sudarsana Reddy, P. and Chamkha, A.J. (2016c), "Soret and dufour effects on MHD convective flow of Al_2O_3-water and TiO_2-water nanofluids past a stretching sheet in porous media with heat generation/absorption", *Advanced Powder Technology*, Vol. 27 No. 4, pp. 1207-1218.

Sudarsana Reddy, P., Sreedevi, P. and Chamkha, A.J. (2017), "MHD boundary layer flow, heat and mass transfer analysis over a rotating disk through porous medium saturated by cu-water and ag-water nanofluid with chemical reaction", *Powder Technology*, Vol. 307, pp. 46-55.

Sundar, L.S., Sharma, K.V., Naik, M.T. and Singh, M.K. (2013), "Empirical and theoretical correlations on viscosity of nanofluids: a review", *Renewable and Sustainable Energy*, Vol. 25, pp. 670-686.

Corresponding author
P. Sudarsan A. Reddy can be contacted at: suda1983@gmail.com

This article has been cited by:

1. Rahimi GheynaniAli, Ali Rahimi Gheynani, Ali AkbariOmid, Omid Ali Akbari, ZarringhalamMajid, Majid Zarringhalam, Ahmadi Sheikh ShabaniGholamreza, Gholamreza Ahmadi Sheikh Shabani, AlnaqiAbdulwahab A., Abdulwahab A. Alnaqi, GoodarziMarjan, Marjan Goodarzi, ToghraieDavood, Davood Toghraie. Investigating the effect of nanoparticles diameter on turbulent flow and heat transfer properties of non-Newtonian carboxymethyl cellulose/CuO fluid in a microtube. *International Journal of Numerical Methods for Heat & Fluid Flow*, ahead of print. [Abstract] [Full Text] [PDF]
2. BakhshiHesam, Hesam Bakhshi, KhodabandehErfan, Erfan Khodabandeh, AkbariOmidali, Omidali Akbari, ToghraieDavood, Davood Toghraie, JoshaghaniMohammad, Mohammad Joshaghani, RahbariAlireza, Alireza Rahbari. Investigation of laminar fluid flow and heat transfer of nanofluid in trapezoidal microchannel with different aspect ratios. *International Journal of Numerical Methods for Heat & Fluid Flow*, ahead of print. [Abstract] [Full Text] [PDF]
3. DehghaniMohammad Sadegh, Mohammad Sadegh Dehghani, ToghraieDavood, Davood Toghraie, MehmandoustBabak, Babak Mehmandoust. Effect of MHD on the flow and heat transfer characteristics of nanofluid in a grooved channel with internal heat generation. *International Journal of Numerical Methods for Heat & Fluid Flow*, ahead of print. [Abstract] [Full Text] [PDF]
4. Ben SalahSana, Sana Ben Salah, Ben HamidaMohamed Bechir, Mohamed Bechir Ben Hamida. Heat transfer enhancement of circular and square LED geometry. *International Journal of Numerical Methods for Heat & Fluid Flow*, ahead of print. [Abstract] [Full Text] [PDF]
5. OzdemirMustafa Bahadir, Mustafa Bahadir Ozdemir, ErgunMustafa Emre, Mustafa Emre Ergun. Experimental and numerical investigations of thermal performance of Al2O3/water nanofluid for a combi boiler with double heat exchangers. *International Journal of Numerical Methods for Heat & Fluid Flow*, ahead of print. [Abstract] [Full Text] [PDF]
6. IzadiMohsen, Mohsen Izadi, MohebbiRasul, Rasul Mohebbi, ChamkhaA., A. Chamkha, PopIoan, Ioan Pop. 2018. Effects of cavity and heat source aspect ratios on natural convection of a nanofluid in a C-shaped cavity using Lattice Boltzmann method. *International Journal of Numerical Methods for Heat & Fluid Flow* **28**:8, 1930-1955. [Abstract] [Full Text] [PDF]